ORIGINAL RESEARCH

Anti-Inflammatory Activation of Phellodendri Chinensis Cortex is Mediated by Berberine Erythrocytes Self-Assembly Targeted Delivery System

Minhua Li[1],*, Zehui Qin[1],*, Qiuxia Yu[2], Ziwei Huang[3], Juanjuan Cheng[1], Linjiang Zhong[1], Yuhong Liu[1], Jianhui Xie[4–6], Yucui Li[1], Jiannan Chen[1], Ruoting Zhan[1], Ziren Su[1]

[1]School of Pharmaceutical Sciences, Guangzhou University of Chinese Medicine, Guangzhou, 510006, People's Republic of China; [2]The Second Clinical College of Guangzhou University of Chinese Medicine, Guangzhou, 510120, People's Republic of China; [3]The First Affiliated Hospital of Chinese Medicine Guangzhou University of Chinese Medicine, Guangzhou, 510120, People's Republic of China; [4]The Second Affiliated Hospital of Guangzhou University of Chinese Medicine, Guangzhou, 510120, People's Republic of China; [5]State Key Laboratory of Dampness Syndrome of Chinese Medicine, The Second Affiliated Hospital of Guangzhou University of Chinese Medicine, Guangzhou, 510120, People's Republic of China; [6]Guangdong Provincial Key Laboratory of Clinical Research on Traditional Chinese Medicine Syndrome, Guangzhou, 510120, People's Republic of China

*These authors contributed equally to this work

Correspondence: Ruoting Zhan; Ziren Su, School of Pharmaceutical Sciences, Guangzhou University of Chinese Medicine, no. 232, Waihuandong Road, Guangzhou Higher Education Mega Center, Guangzhou, 510006, People's Republic of China, Email zhanrt@gzucm.edu.cn; suziren@gzucm.edu.cn

Background: Berberine (BBR) is the primary active component of Phellodendri Chinensis Cortex (PCC), which has been traditionally used to treat inflammatory diseases. However, the discrepancy between its low bioavailability and significant therapeutic effect remains obscure. The purpose of this study was to explore the previously unsolved enigma of the low bioavailability of BBR and its appreciable anti-inflammatory effect to reveal the action mechanism of BBR and PCC.
Methods: The quantitative analysis of BBR and its metabolite oxyberberine (OBB) in blood and tissues was performed using high-performance liquid chromatography to investigate the conversion and distribution of BBR/OBB mediated by erythrocytes. Routine blood tests and immunohistochemical staining were used to explore the potential relationship between the amounts of monocyte/macrophage and the drug concentration in erythrocytes and tissues (liver, heart, spleen, lung, kidney, intestine, muscle, brain and pancreas). To comparatively explore the anti-inflammatory effects of BBR and OBB, the acetic acid-induced vascular permeability mice model and lipopolysaccharide-induced RAW 264.7 macrophages were employed.
Results: Nearly 92% of BBR existed in the erythrocytes in rats. The partition coefficient of BBR between plasma and erythrocytes (Kp/b) decreased with time. OBB was found to be the oxidative metabolite of BBR in erythrocytes. Proportion of BBR/OBB in erythrocytes changed from 9.38% to 16.30% and from 13.50% to 46.24%, respectively. There was a significant relationship between the BBR/OBB concentration in blood and monocyte depletion after a single administration of BBR. BBR/OBB was transported via erythrocytes to various tissues (liver, kidney, spleen, lung, and heart, etc), with the liver achieving the highest concentration. OBB exhibited similar anti-inflammatory effect in vitro and in vivo as BBR with much smaller dosage.
**Conclusion:** BBR was prodominantly found in erythrocytes, which was critically participated in the biodistribution, pharmacokinetics, metabolism and target delivery of BBR and its metabolite. The anti-inflammatory activity of BBR and PCC was intimately associated with the metabolism into the active congener OBB and the targeted delivery to monocytes/macrophages mediated by the erythrocytes.
Keywords: erythrocytes, Phellodendri Chinensis Cortex, transformation, berberine, anti-inflammation

Introduction

Phellodendri Chinensis Cortex (PCC, Figure 1), known as "Chuan HuangBai" in China, is a commonly used Chinese medicinal herb derived from the dried bark of *Phellodendron chinense* Schneid.[1] PCC has the function of clearing heat,

Graphical Abstract
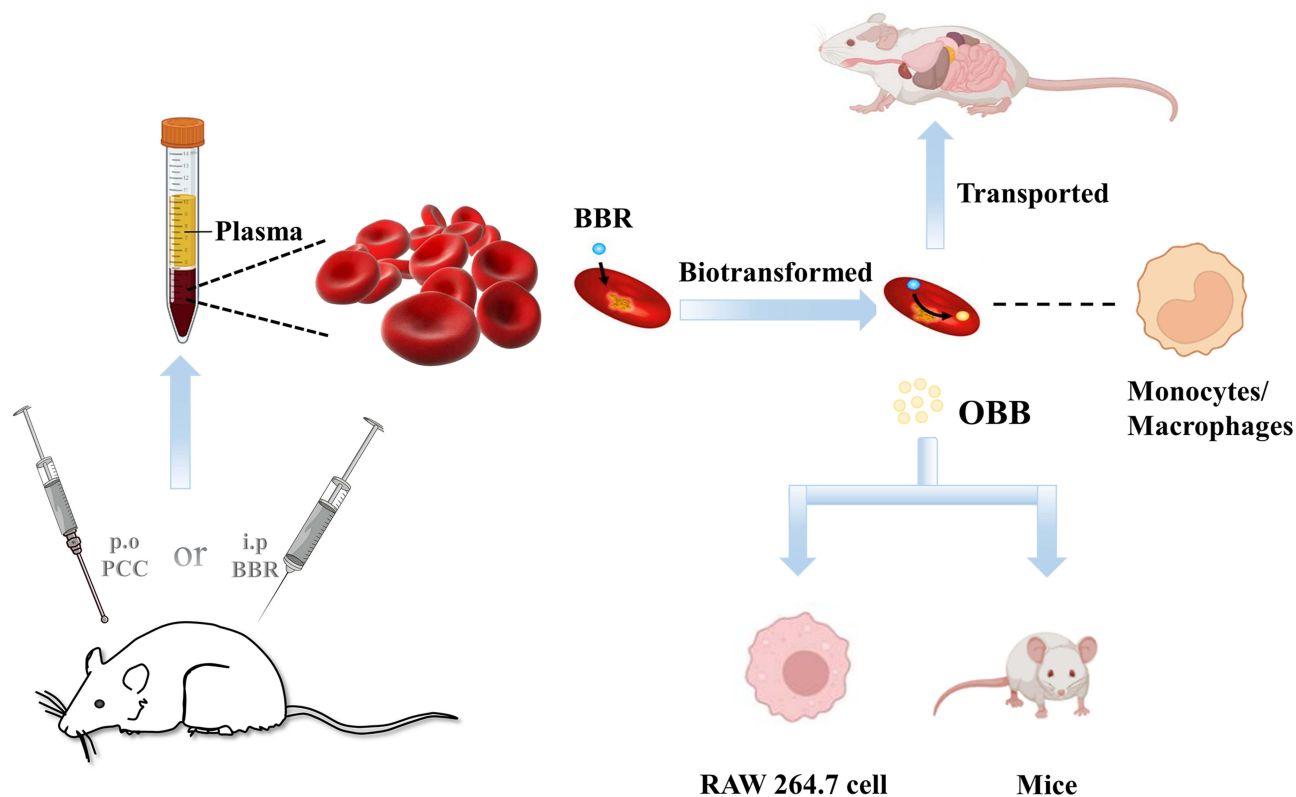
eliminating dampness, purging fire, and removing toxicity, and is traditionally applied in the treatment of inflammatory diseases.[2,3] Protoberberine alkaloids are regarded as the major active components of PCC. Particularly, berberine (BBR, Figure 1), the most predominant protoberberine alkaloid and one of the quality control markers of PCC, is largely accountable for the potential therapeutic effects of PCC. BBR has been found to possess appreciable therapeutic activities in inflammation-related disorders and illnesses such as inflammasome-involved kidney injury,[4] ulcerative colitis,[5] and osteoarthritis.[6]

However, the extremely low plasma concentration and oral bioavailability (0.36%) of BBR are insufficient in experimental or clinical settings to yield the effects as observed under experiments, which raises challenges to adequately explain its exceptional anti-inflammatory potency in clinical trials.[7,8] The majority of researches on BBR metabolism

Phellodendron Chinese Schneid   Phellodendri Chinensis Cortex   Berberine   Oxyberberine
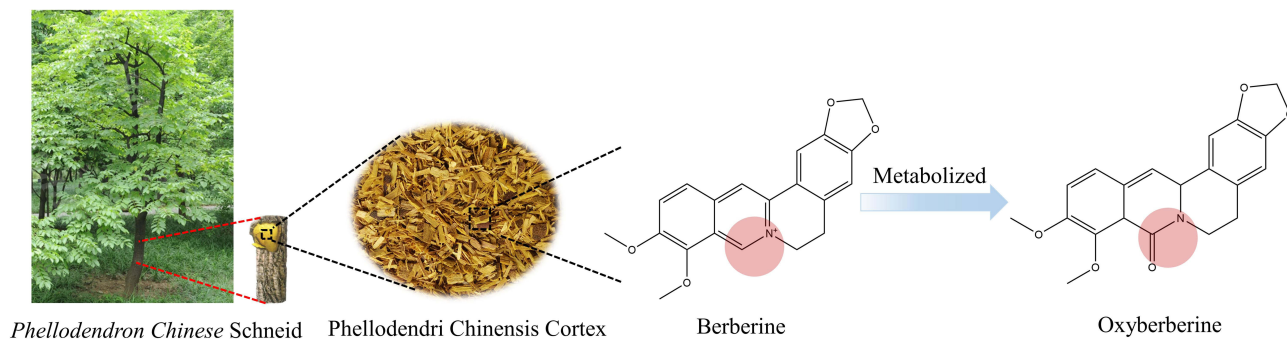
Figure 1 The relationship between Phellodendri Chinensis Cortex (PCC), berberine (BBR) and oxyberberine (OBB).

were concentrated on the intestinal tract and hepatic system. Plenty of pharmacokinetic-pharmacodynamic studies on BBR are concentered on its concentration and metabolites in plasma; however, it was not sufficient to explain the contradiction between its low plasma concentration and high potency.

Erythrocyte metabolism is an important metabolic pathway that is easily ignored. Erythrocytes are the main cells in blood circulation, which provide the extraordinary vehicles for the dissemination of drugs in blood circulation.[9] Hemoglobin (Hb), the most abundant protein in the blood, possessed the properties of catalase thus catalyzing the oxidation reaction.[10,11] In our recent work, we have found that BBR could bind to Hb assembly and form a BBR-erythrocytes drug delivery system.[12] Furthermore, oxyberberine (OBB, Figure 1), whose C-9 position is oxidized to a carbonyl group to form an amide ring with 8-N atoms, has been identified as the essential metabolite after intravenous administration of BBR in our previous study.[13] Erythrocytes are equipped with various reactive oxygen species and enzymes to catalyze drug metabolism, particularly drug oxidation.[14,15] Furthermore, erythrocytes identify the drug molecules and deliver them to the target site, resulting in the hepatic accumulation.[16] Herewith, erythrocytes have currently been deemed as the excellent site-targeted delivery system.[17,18] However, the potentially important role that erythrocytes play in the metabolism and disposition of BBR may have been ignored.

On the basis of our preliminary study, erythrocytes are hypothesized as the other metabolic site of BBR besides intestinal tract and liver. As part of our ongoing search and to test our hypothesis, the present endeavor has been devoted to exploring the role of erythrocytes in the metabolism and delivery of BBR to reveal the anti-inflammatory mechanism of PCC. Our study furnished a novel version to interpret the paradox between excellent anti-inflammatory effect and extremely low absolute bioavailability of BBR from the perspective of the erythrocyte-drug delivery system and the quantitative-effect relationship. The results will contribute to a better understanding of the underlying material basis of the anti-inflammatory effects of BBR and PCC, and are also envisaged to provide a paradigm for erythrocytes in drug metabolism and provide an enlightenment for the study on activity presentation of Chinese medicine from the erythrocyte drug carrier system.

Materials and Methods

Chemicals and Reagents

PCC and berberine hydrochloride (purity >98%) were provided by Guangzhou Herbal Medicine Company (Guangzhou, China) and Chengdu HerbPurity CO., Ltd. (Chengdu, China), respectively. OBB (purity >98%) was synthesized and identified following our preceding study.[19] High-performance liquid chromatography (HPLC) – grade acetonitrile was bought from Guangzhou Lubex Biological Technology Co., Ltd. (Guangzhou, China). Trifluoroacetic acid (TFA) was obtained from Shanghai Aladdin Biochemical Technology Co., Ltd. (Shanghai, China). Deionized distilled water was supplied by China Resources C'estbon Beverage (China) Co., Ltd. Lipopolysaccharide (LPS), dimethyl sulfoxide (DMSO) and Evans blue were obtained from Sigma-Aldrich (St. Louis, MO, USA). Enzyme-linked immunosorbent assay (ELISA) kits (TNF-α, IL-6, and IL-18) were purchased from Shanghai Enzyme-linked Biotechnology Co., Ltd. (Shanghai, China). BCA protein assay kit was obtained from Shanghai BestBio Biological Technology Co., Ltd. (Shanghai, China). Other reagents were of the highest purity and analytical grade.

Preparation of PCC Extract

The PCC extraction method was employed according to Wang et al with some modifications.[20] PCC was crushed into powder (300 g) and extracted with 1200 mL 80% ethanol (1:4, w/v) solution at 75 °C for 3 h, which was performed three times. The PCC extract was then filtered and merged for rotatory evaporation till no alcohol taste was found. Finally, the residue was suspended in 0.9% saline. BBR content was measured by HPLC (LC-20AT, Shimadzu, Kyoto, Japan), and the final concentration of BBR was 40 mg/mL.

Animals

Male Sprague Dawley (SD) rats (220–240g) and Kunming mice (18–22g) of both sexes were purchased from the Medical Experimental Animal Center of Guangzhou University of Chinese Medicine. The experimental procedures were

conducted under the approval of the Institutional Ethics Committee of Guangzhou University of Chinese Medicine (Ethics No. 20210609001) and carried out in accordance with the Guidelines on the Care and Use of Laboratory Animal issued by the Chinese Council on Animal Research and the Guidelines of Animal Care. Animals were housed under specific pathogen-free conditions of 22 ± 2 °C and $55 \pm 2\%$ humidity with a 12-h light/dark cycle, and fed with conventional food and water *ad libitum*.

Pharmacokinetic Study

For the analysis of pharmacokinetics of PCC in vivo, six SD rats were orally administered with a single dose of PCC extract, which corresponded to an equivalent dose of BBR (100 mg/kg) via intragastric administration. The blood was collected from the orbital sinus venous plexus of rats in the sampling vessel which was infiltrated with heparin sodium at 0.083, 0.167, 0.25, 0.5, 1, 2, 2.5, 4, 5, 6, 7, 8, 12, and 24 h.

The blood samples were treated according to our previous study with some modifications.[13] The whole blood stood at 4 °C for 2 h and was then centrifuged at 2500 rpm for 10 min to obtain plasma from upper layer and erythrocytes from lower layer. And, 250 μL of plasma was mixed with the internal standard (I.S.), precipitated by 1 mL acetonitrile, and subsequently centrifuged at 8000 rpm for 10 min at 4 °C. The supernatant was collected, dried in an electric oven, and redissolved with 200 μL methanol. Erythrocyte samples were washed with normal saline (1:5, v/v) three times mixed with 15% HCl and allowed to react at 60 °C for 6 h to hydrolyze the protein. After centrifugation at 8000 rpm for 10 min, the supernatant was loaded into the pre-treated SPE column and eluted with three times of methanol. The eluents were concentrated and redissolved in 200 μL acetonitrile. All the samples were filtered through a 0.22-μm filter membrane before HPLC analysis.

HPLC Analysis

HPLC system (LC-20AT, Shimadzu, Kyoto, Japan) was used to determine the concentrations of BBR and OBB in the plasma and erythrocytes. Phenomenex C18 column (250 × 4.6 mm, 5 μm) was employed for separation analysis. The mobile phases were consisted of solvent A (water with 0.1% trifluoroacetic acid) and solvent B (acetonitrile). The gradient elution settings were as follows: 90–10% A for 0–20 min, and 10–90% A for 20–30 min. The UV detection wavelength was 345 nm. Then, 10 μL samples were injected for determination, and the flow rate was 1.0 mL/min.

Method Validation

Selectivity was determined to detect the interferences of analytes and piperine (internal standard, IS) at the retention time by evaluating blank whole blood samples from six rats as well as whole blood samples spiked with analytes. Linearity was determined by plotting the peak area ratio of analytes/IS against the concentrations of analytes in plasma and erythrocytes through least-squares linear regression using $1/x^2$ as a weight factor. The lower limit of quantification (LLOQ) was defined as the lowest concentration with a signal-to-noise ratio of at least 10.

The accuracy, precision, and recovery of the method were tested with the quality control (QC) samples prepared within the calibration range. Six replicates of each QC sample were determined to acquire the mean concentrations and then compared with the nominal concentrations to evaluate the accuracy, inter- and intra-day precision. The stability of samples was evaluated after storage at room temperature for 4 h, at −10 °C for 1 month, and after three freeze–thaw cycles from −80 °C to room temperature. The relative recovery of each analyte was evaluated by comparing the average peak areas of the QC samples after extraction with the average peak areas of spiked-after extraction samples, representing the 100% recovery value.

Bioconversion of BBR by Erythrocytes in vivo

BBR was dissolved in normal saline for injection. The BBR solution was intraperitoneally administered to the rats at a volume of 2.5 mg/kg body weight. Whole blood was collected from the fundus venous plexus at 0.5, 1, and 2 h after administration and treated according to Pharmacokinetic study as mentioned above.

Incubation of BBR and OBB in vitro

The in vitro study was performed to further explore the role of erythrocytes on the transportation and existing form of BBR. BBR and OBB were added to the blank whole blood and plasma samples respectively to obtain a final level of 10 μM. Post incubation at 37 °C for 2 h, 4-fold acetonitrile was added to the incubation system to terminate the reaction and then manipulated following Pharmacokinetic study as described above. In addition, another whole blood sample was hydrolyzed by HCl and then treated according to Pharmacokinetic study as mentioned above. Finally, the contents of BBR and OBB in whole blood and plasma samples were comparatively quantified using HPLC.

Routine Blood Test: Assessing the Relationship Between the Drug Concentration in Erythrocytes and the Amounts of Hemocytes

The blood test was performed as described in the literature[21] with minor modifications. The amounts of erythrocyte, leukocyte, lymphocyte, neutrophil, monocyte, and Hb were counted and recorded.

Tissue Distribution Mediated by Erythrocytes

SD rats divided into four groups (n = 6) were orally administered a single dose of 400 mg/kg BBR and sacrificed at 1, 2, 4, and 6 h respectively after being anesthetized by ether. Afterwards, the liver, kidney, heart, spleen, lung, intestine, pancreas, brain, and muscle were removed rapidly, washed with normal saline, cut into small pieces, and dried with filter paper. Then, 0.25 g of these samples were put into the centrifuge tubes and homogenized with a homogenizer (Wuhan Servicebio Technology Co., Ltd.) with the addition of acetonitrile at a ratio of 1:4 (w/v). Centrifugation was conducted at a speed of 8000 rpm for 10 min, and the supernatant was dried in an electric oven, redissolved with 200 μL methanol and filtered with 0.22-μm nylon membrane prior to injection into HPLC.

Immunohistochemical Staining: Assessing the Relationship Between the Tissue Distribution and the Amounts of Macrophages

Immunohistochemistry was used to characterize the macrophages (CD68, dilution 1:500, Servicebio, Wuhan, China). Specimens of the normal rat tissues (liver, spleen, kidney, heart, lung) were fixed in 4% neutral formalin solution and then routinely processed as previously described[22] with minor modifications. Under the observation at high magnification (×400) from five randomly selected sampling areas, CD68^{+} macrophages were quantified using images captured with a digital camera system and calculated by using Image-Pro Plus software (Media Cybernetics, MD, USA). Results were expressed as the average number of CD68^{+} cells per image.

Alteration of Anti-Inflammatory Activity of BBR

Cell Culture and Treatment

The murine macrophage RAW 264.7 cells were purchased from the American Type Culture Collection (Rockville, MD, USA). Cells were incubated in Dulbecco's Modified Eagle Medium (DMEM) supplemented with 10% fetal bovine serum and 1% penicillin-streptomycin in a humidified incubator with an atmosphere consisting of 95% air and 5% CO_2 at 37 °C until 70–80% confluency before drug treatment. RAW 264.7 cells were pre-treated with BBR or OBB for 4 h and subjected to stimulation of LPS for another 24 h.

Cell Viability Assay

RAW 264.7 cells were seeded into the 96-well plate (1×10^5 cells/well, 100 μL medium/well) for 24 h. Cells were treated with BBR (80, 40, 20, 10, 5, 2.5 μM), or OBB (80, 40, 20, 10, 5, 2.5 μM) with or without LPS. After incubation at 37 °C for 24 h, 10 μL cell counting kit-8 solution was added to each well and incubated for 0.5 h. The absorbance was detected at 450 nm by a microplate analyzer.

ELISA for TNF-α, IL-6, and IL-18 Levels

Cells were seeded into 12-well plate (1×10^5 cells/well, 500 μL medium/well) and pre-treated with OBB (0.1, 0.2, 0.4 μM) and BBR (5 μM) for 4 h, then treated with LPS (1 μg/mL) for an additional 24 h. The supernatant was extracted

from each well for the ELISA test kits to determine the content of inflammatory cytokines according to the manufacturer's instructions. The dosages of BBR and OBB were employed based on our prior trial.

Acetic Acid-Induced Vascular Permeability Test

The assay was performed according to the previous study[23] with some modifications. During the experiment, mice were randomly divided into six groups (5 male and 5 female per group). The treatment groups were orally administered with different doses of OBB (1, 2, 4 mg/kg) and BBR (4 mg/kg, positive drug) for 7 consecutive days. The normal group and the model group were given normal saline as a control. One hour after the last administration, mice were intravenously injected with 1% Evans blue in saline (10 mL/kg) and then given an intraperitoneal injection of 0.6% (v/v) acetic acid (10 mL/kg). Mice were sacrificed after 20 min. The abdominal cavity was washed with 5 mL ice-cold normal saline. The peritoneal exudate was collected after centrifuged at 3000 rpm for 10 min. The absorbance of supernatants was measured at 590 nm using a SHIMADZU UV2600 UV–VIS spectrophotometer (Shimadzu, Tokyo, Japan). The vascular permeability was evaluated by quantifying the infiltration of Evans blue dye into the peritoneal cavity.

Statistical Analysis

Data are expressed as mean ± standard error of the mean (S.E.M.). Shapiro–Wilk test was applied to assess the normal distribution of the data. Student's t-test or One-way ANOVA/Dunnett's t-test was used for the assessment of significance between two groups or multiple groups. Statistical analysis was performed by SPSS software (version 26.0; SPSS Inc, Chicago, IL, USA). Values of $p < 0.05$ or $p < 0.01$ were considered statistically significant.

Results
Preparation of PCC Extract

As shown in Figure 2, the content of BBR in PCC was over 3.0%, which met the requirement for the extract of PCC according to Chinese Pharmacopeia (2020 edition). OBB in PCC extract was beyond the limit of detection (LOD) of HPLC.
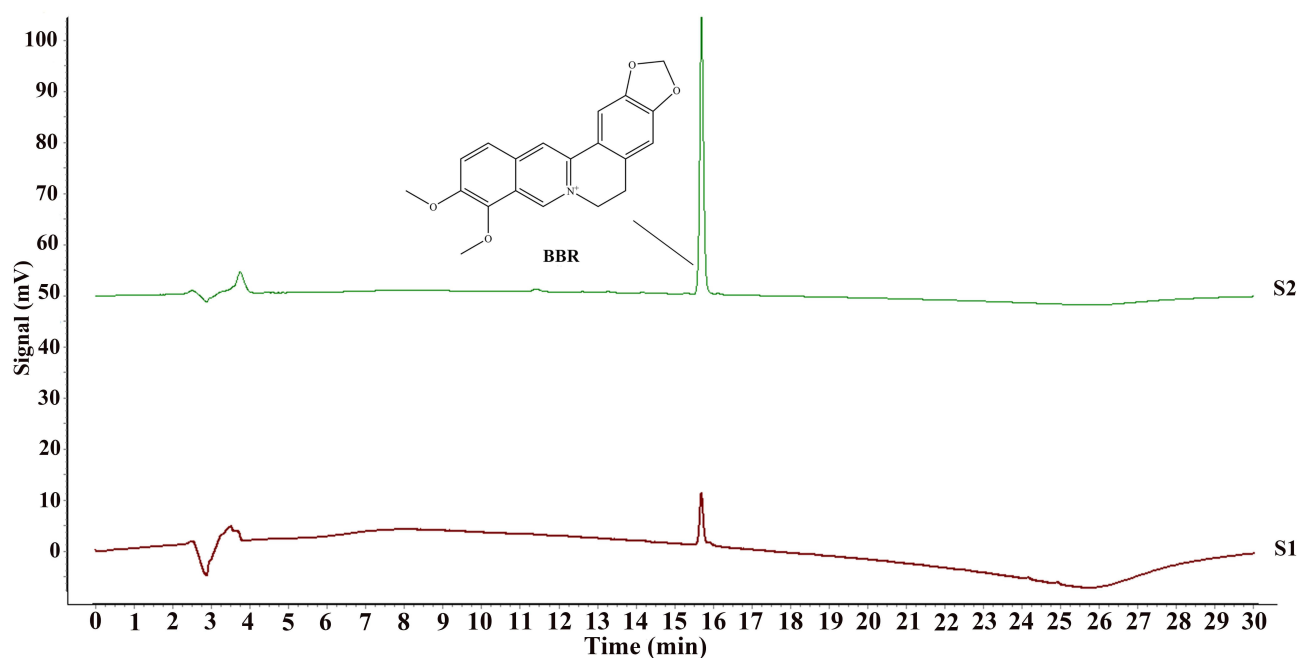
Figure 2 BBR in PCC extract was analyzed using HPLC. (S1) PCC extract with 95% ethanol. The purity of BBR was over 95% and the content of BBR was over 3.0%. (S2) BBR standard solution.

HPLC Method Validation

The above HPLC method was validated for simultaneous quantitative detection of BBR and OBB in rat plasma and erythrocytes. Some representative HPLC images of samples are shown in Figure 3. Under this developed method, BBR, OBB, and IS can be separated well from each other and no endogenous substances affected the detection of the target peaks. The HPLC chromatogram indicated that OBB was the metabolite of BBR rather than the chemical oxidative product of BBR. Calibration curves were found to be linear over the concentration ranging from 0.049 to 12.500 μg/mL for BBR and OBB, both with correlation coefficient over 0.9995.

The accuracy and precision for the measurement of BBR and OBB in rat plasma and erythrocytes are shown in Table 1. The relative errors (RE%) of accuracy were within 15%, and the relative standard deviations (RSD%) of intra-, inter-day precision remained within 15%. The recovery rates were in the range of 85–115%. As tabulated in Table 2, RSD% of stability of the analytes was lower than 15%, indicating that samples were stable during storage at room temperature for 4 h, at −10 °C for 1 month and following three freeze–thaw cycles from −80 °C to room temperature, respectively. Therefore, the linearity, accuracy, precision, recovery, and stability of biological samples satisfied the standards for quantitative analysis.

Pharmacokinetic Study

As shown in Figure 4A, post oral administration of PCC, the T_{max} of BBR in rat blood was 1 h and subsequently maintained at a low plasma concentration for 24 h. Of note, compared to BBR in plasma, the area under the blood drug concentration–time curves (AUC_{0-t}) and the peak concentration (C_{max}) for the concentration of BBR in erythrocytes were dramatically elevated ($p < 0.01$). It was interesting to find that OBB was detected after administration of PCC. Figure 4B indicates that AUC_{0-t} and C_{max} of OBB in plasma were both much lower than those in erythrocytes. Either in plasma or erythrocytes, the concentration and AUC_{0-t} of OBB were lower than those of BBR, which indicated OBB was presented at a merely low concentration and the major constituent of PCC in vivo was BBR. The second concentration peak of OBB appeared 3 h later than BBR, suggesting that erythrocytes might perform a potential role in retarding drug release.
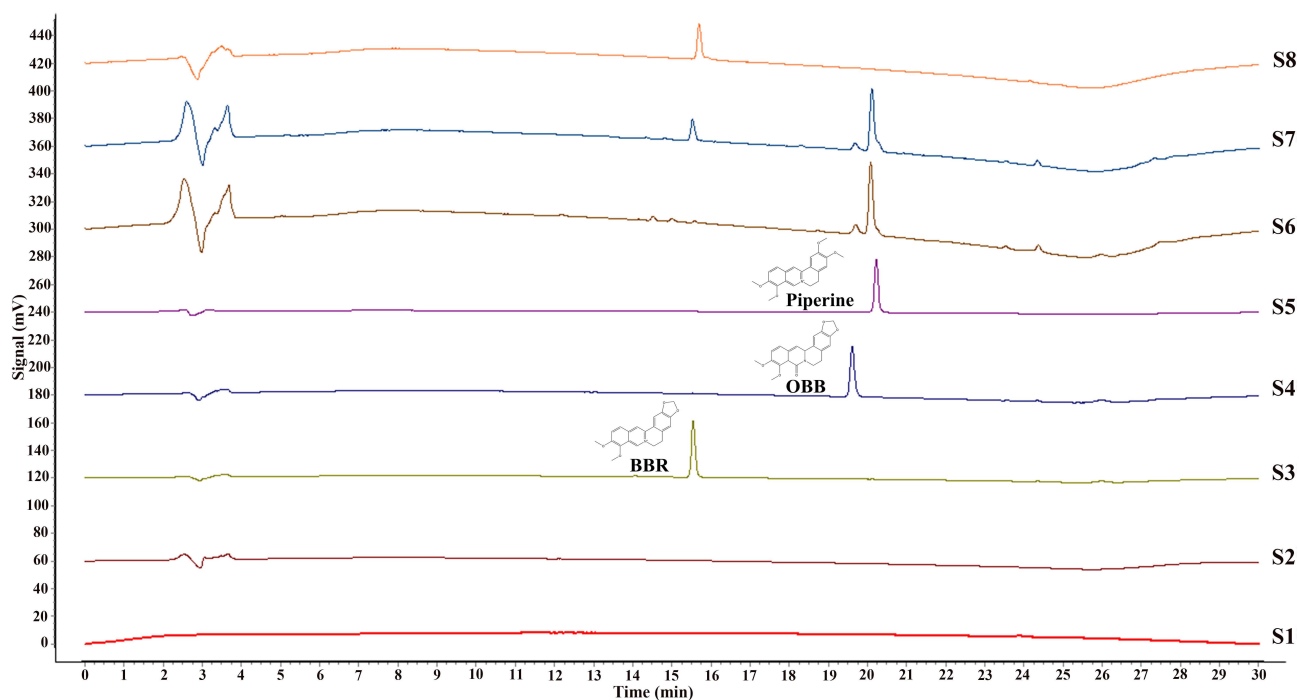
Figure 3 HPLC chromatograms of blood samples with BBR and OBB. (S1) Blank whole blood treated with acetonitrile precipitation. (S2) Blank whole blood hydrolyzed by HCl. (S3–S5) Whole blood spiked with BBR, OBB, and IS standard solutions. (S6) Plasma samples obtained following intraperitoneal injection of BBR in 0.5 h. (S7) Erythrocyte samples acquired after intraperitoneal administration of BBR in 0.5 h. (S8) BBR hydrolyzed by HCl.

Table 1 Accuracy, Recovery, and Intra-Day and Inter-Day Precisions of BBR and OBB in Plasma and Erythrocytes (n = 6)

| Analytes	Nominal Concentration (µg/mL)	Plasma				Erythrocytes			
		Accuracy-RE (%)	Recovery (%)	Intra-Day RSD (%)	Inter-Day RSD (%)	Accuracy-RE (%)	Recovery (%)	Intra-Day RSD (%)	Inter-Day RSD (%)
BBR	0.30	2.34 ± 0.74	99.24 ± 1.23	2.89	4.16	2.37 ± 0.60	100.95 ± 1.14	3.66	4.51
	1.56	1.83 ± 0.58	98.23 ± 0.62	0.94	1.49	1.08 ± 0.39	100.68 ± 0.54	0.62	1.13
	6.25	0.12 ± 0.03	99.97 ± 0.06	0.22	0.15	0.18 ± 0.09	99.94 ± 0.12	0.14	0.18
OBB	0.30	2.77 ± 0.61	102.70 ± 0.67	1.99	4.23	2.90 ± 0.78	100.43 ± 1.50	3.46	4.41
	1.56	2.05 ± 0.69	98.33 ± 0.87	0.71	1.43	1.06 ± 0.34	100.64 ± 0.51	0.76	1.20
	6.25	0.22 ± 0.10	100.21 ± 0.11	0.15	0.20	0.33 ± 0.11	100.07 ± 0.18	0.23	0.13

Notes: Data are expressed as mean ± S.E.M. (n = 6).

Table 2 The Stability (RSD %) of BBR and OBB in Plasma and Erythrocytes Under Three Different Storage Conditions (n = 6)

Analytes	Nominal Concentration (µg/mL)	Plasma			Erythrocytes		
		Room Temp. for 4 h	Frozen for 1 Month (−10 °C)	Three Freeze–Thaw cycles	Room Temp. for 4 h	Frozen for 1 Month (−10 °C)	Three Freeze–Thaw Cycles
BBR	0.30	5.36	7.72	9.35	4.97	7.47	9.13
	1.56	1.14	1.92	1.63	1.68	2.40	2.02
	6.25	0.74	1.27	1.15	0.92	1.15	0.97
OBB	0.30	3.26	8.60	8.86	4.78	6.63	6.39
	1.56	1.32	1.62	2.14	1.07	2.06	2.82
	6.25	0.24	0.57	0.68	0.50	0.77	1.71

Determination of BBR and OBB in vitro

To explore the effect of erythrocytes on the existing forms of BBR and OBB, different methods were used to treat the blood samples incubated with BBR/OBB. As tabulated in Table 3, in comparison to the plasma sample, the concentrations of BBR/OBB in whole blood were significantly decreased after treatment with acetonitrile. The result indicated that BBR entered into the erythrocytes, and BBR and OBB bound with Hb. The levels of BBR and OBB in the whole blood treated with HCl were significantly higher than those treated with acetonitrile since Hb was hydrolyzed and the drugs were released.
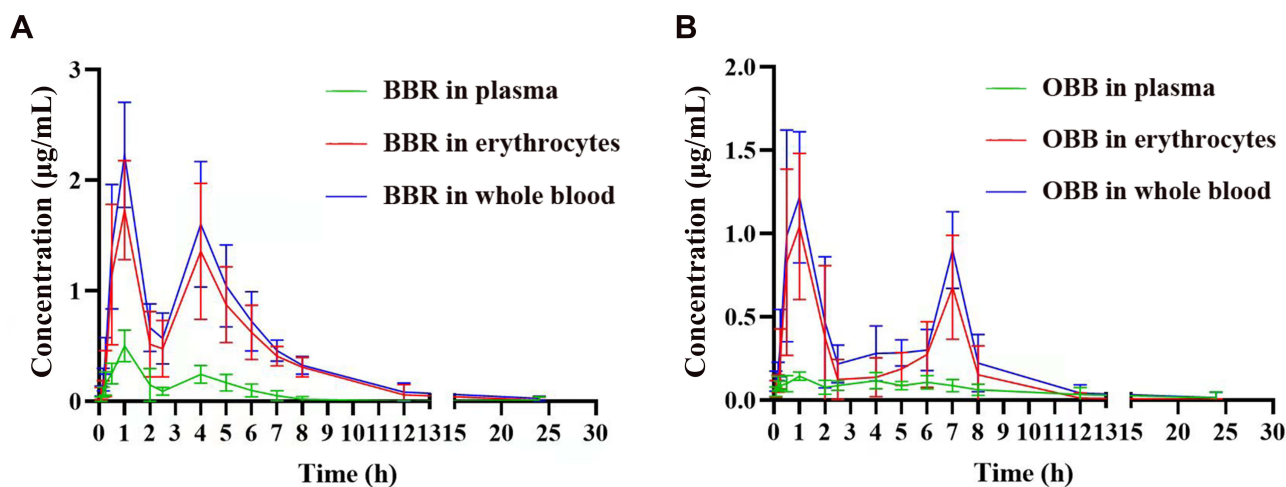
Figure 4 Blood concentration–time curves of BBR and OBB post oral administration of PCC. Blood concentration–time curve of BBR (**A**) and OBB (**B**). Data are expressed as mean ± S.E.M. (n = 6).
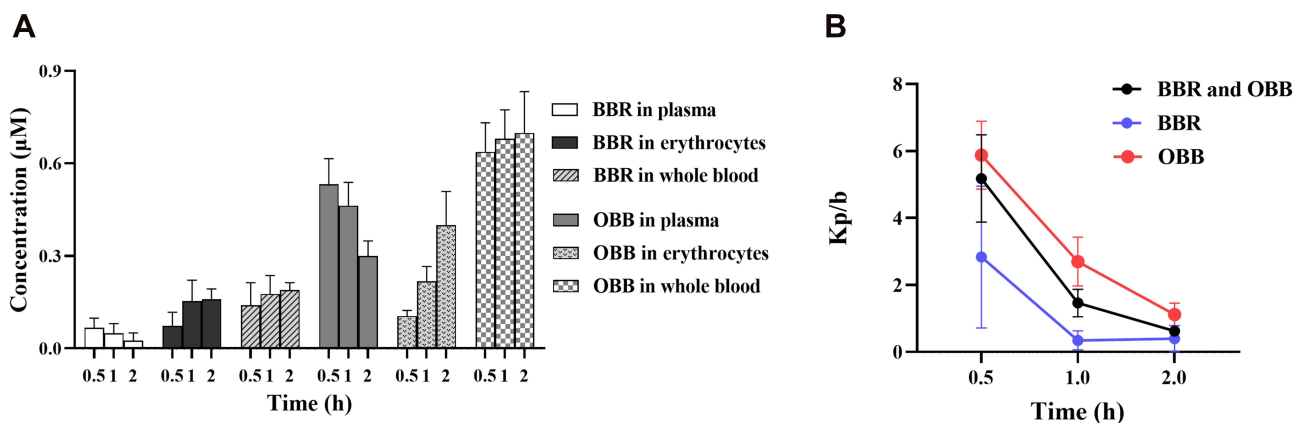
Table 3 The Concentration of BBR and OBB in Plasma and Whole Blood After Incubation in vitro in 2 h (n = 6)

| Sample	BBR			OBB		
	Treatment	Concentration Added (μM)	Concentration Found (μM)	Treatment	Concentration Added (μM)	Concentration Found (μM)
Plasma	Acetonitrile precipitation	10	9.62 ± 0.13	Acetonitrile precipitation	10	9.46 ± 0.10
Whole Blood	Acetonitrile precipitation		5.52 ± 0.14**	Acetonitrile precipitation		5.70 ± 0.08**
Whole Blood	HCl hydrolysis		9.30 ± 0.13##	HCl hydrolysis		9.34 ± 0.16##

Notes: Data are expressed as mean ± S.E.M. (n = 6). **$p < 0.01$ vs concentration found in plasma treated with acetonitrile precipitation. ##$p < 0.01$ vs concentration found in whole blood treated with acetonitrile precipitation.

Effect of Erythrocytes on the Metabolic Feature of BBR

Concentrations and partition coefficients of BBR and OBB in plasma and erythrocytes were revealed in Figures 5 and 6, respectively. The concentration of BBR was 0.067 ± 0.031, 0.049 ± 0.032, 0.025 ± 0.025 μM in plasma respectively and 0.073 ± 0.044, 0.154 ± 0.068, 0.160 ± 0.033 in erythrocytes respectively at 0.5, 1 and 2 h. The partition coefficient between plasma and erythrocytes ($K_{p/b}$) of BBR and OBB showed a downward trend, indicating that both BBR and OBB in plasma decreased gradually and had an opposite tendency in erythrocytes. OBB was detected after intraperitoneal injection of BBR and the proportion of OBB in erythrocytes was 13.5%, 23.32%, and 46.24% respectively at 0.5, 1 and 2 h, indicative of an increasing trend in rats in vivo.

Figure 5 (**A**) Concentrations of BBR and its metabolite OBB measured in rats after intraperitoneal injection of BBR at the dose of 2.5 mg/kg body weight at 0.5, 1, and 2 h. (**B**) Trend variation of plasma/erythrocytes partition coefficients of BBR and OBB in vivo at 0.5, 1 and 2 h. Data are expressed as mean ± S.E.M. (n = 6).
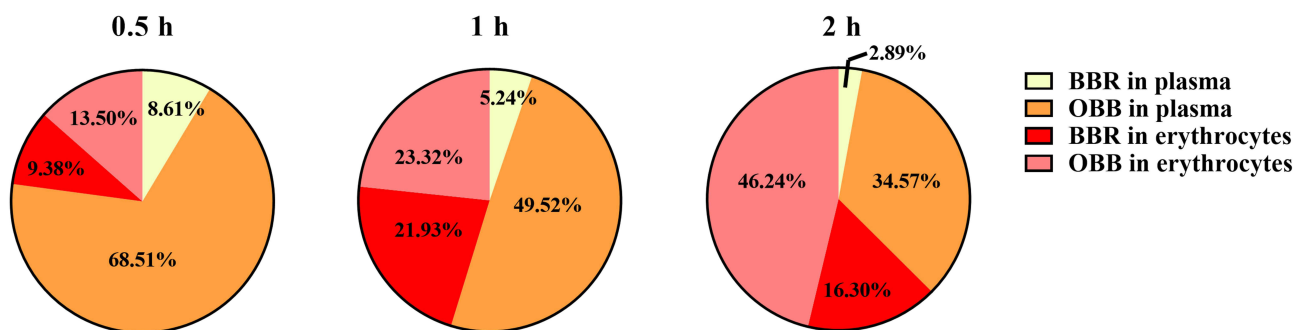
Figure 6 The proportion of BBR and OBB in whole blood after intraperitoneal injection of BBR at the dose of 2.5 mg/kg at 0.5, 1, and 2 h.

Relationship Between the Drug Concentration in Erythrocytes and the Amounts of Monocytes

The changes in the number of rat hemocytes after intraperitoneal injection of BBR at 0.5, 1, 2 h were shown in Figure 7. The amounts of erythrocytes had no significant changes during this period (Figure 7A). Total leukocyte count and Hb had a significant reduction at 2 h (Figure 7B and C) and the number of monocytes was found to decrease markedly in 1 and 2 h (Figure 7C) compared to those of the normal group. Pearson correlation analysis showed that the numbers of monocytes in the peripheral blood were highly related to the concentrations of BBR and OBB in erythrocytes ($r = -0.970$, $p = 0.030$).
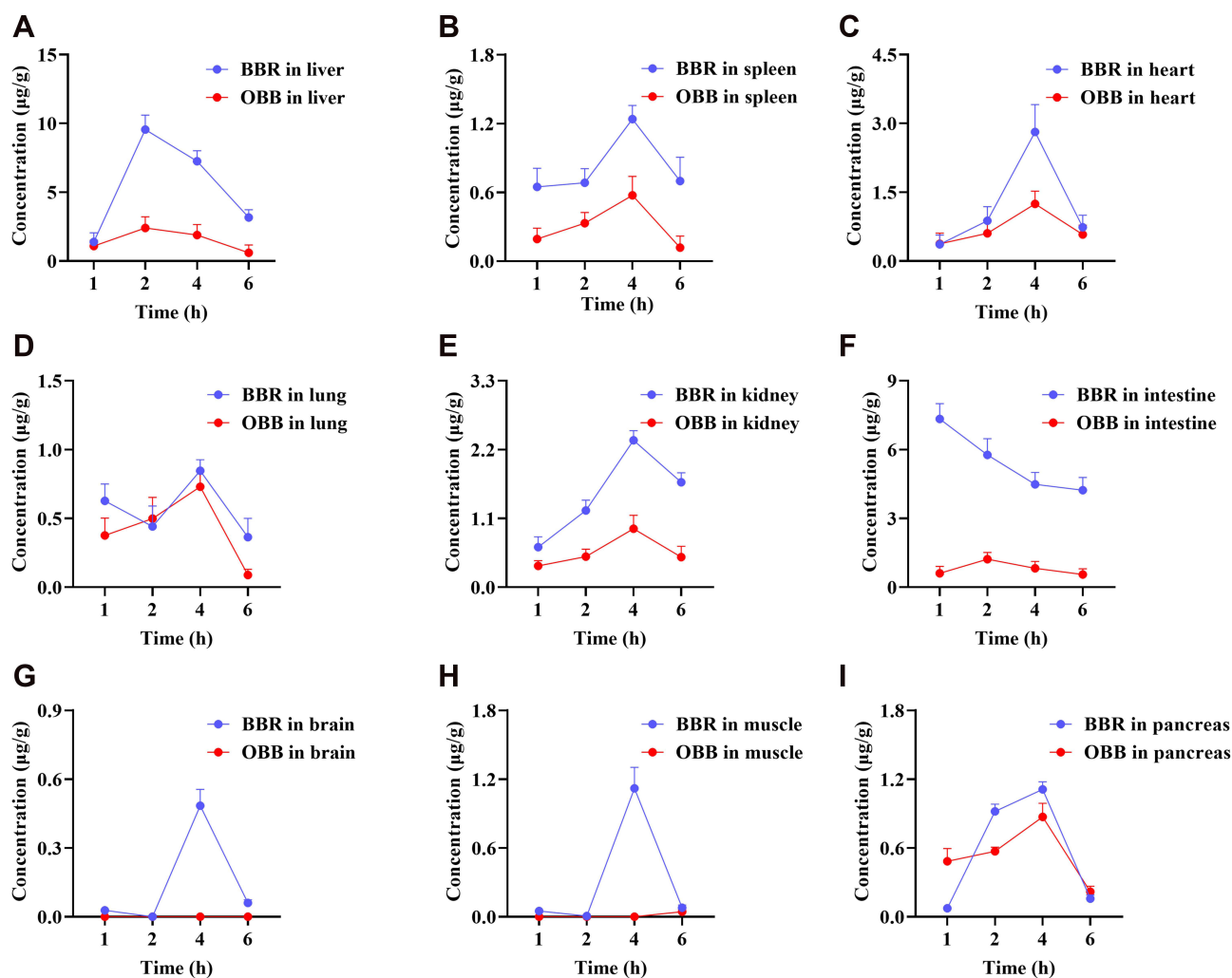
Tissue Distribution

As shown in Figure 8, BBR was found to spread throughout the body including liver, kidney, heart, spleen, lung, intestine, pancreas, brain, and muscle within 6 h. BBR had a maximum concentration in the intestine, followed by the liver, indicating that BBR was absorbed from the intestine into the blood and mainly transported to the liver then to other organs via systemic circulation. OBB, a metabolite of BBR, was found in the liver, kidney, heart, lung, intestine, and pancreas, and was barely detectable in the brain and muscle after oral administration of BBR. OBB was transported to various target organs via erythrocytes after absorption, and the liver was the main target organ.

Evaluation of Immunohistochemistry

The numbers of CD68^{+} macrophages in different tissues were yielded by averaging the quantities of positively stained cells at high magnification ($\times 400$) from each image. Of these five tissues, the spleen possessed the largest number of CD68^{+} macrophages, followed by the liver, lung, heart, and the least abundance of CD68^{+} cells was present in the kidney
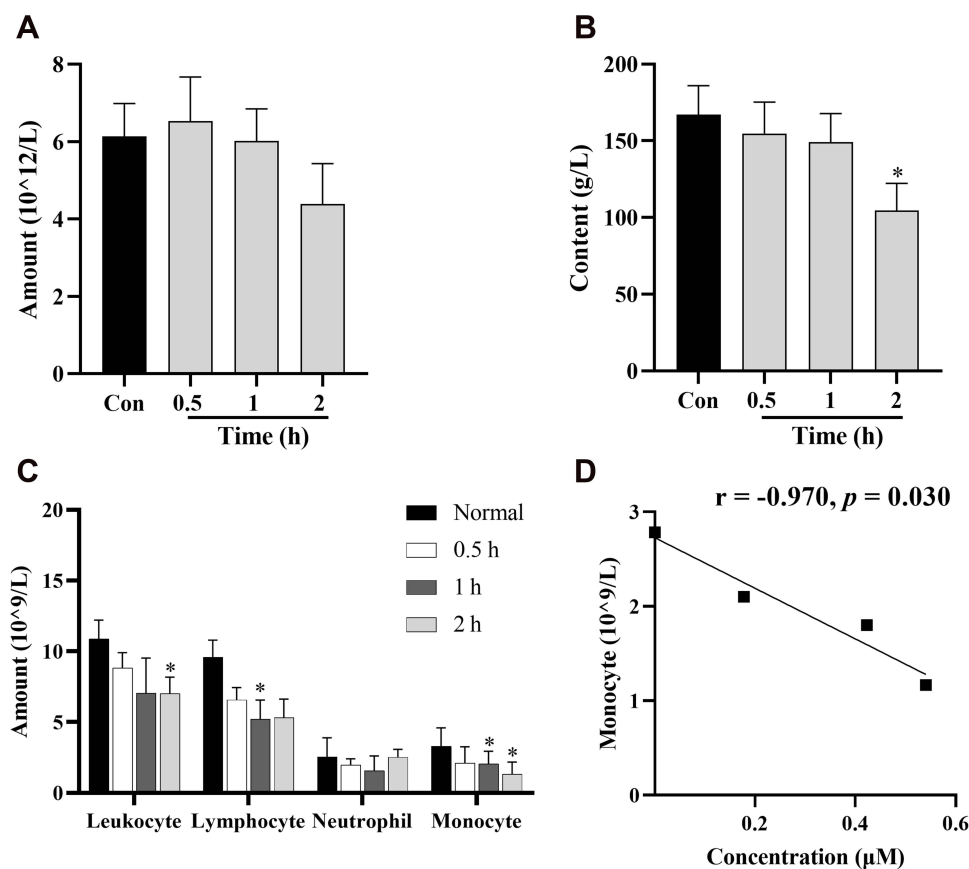
Figure 7 Routine blood tests in rats after intraperitoneal injection of BBR at 0.5, 1, and 2 h at the dose of 2.5 mg/kg body weight. Changes in numbers of erythrocytes (**A**), Hb (**B**), and immune cells (**C**). (**D**) Significant correlations between drug concentration in erythrocytes and the amounts of monocytes. Data are presented as mean ± S.E.M. (n = 3). *$p < 0.05$ vs the normal group.

Figure 8 Distribution profiles of BBR and OBB in the liver (**A**), spleen (**B**), heart (**C**), lung (**D**), kidney (**E**), intestine (**F**), brain (**G**), muscle (**H**), and pancreas (**I**) in rats post oral administration of 400 mg/kg BBR at 1, 2, 4, and 6 h. Data are presented as mean ± S.E.M. (n = 6).
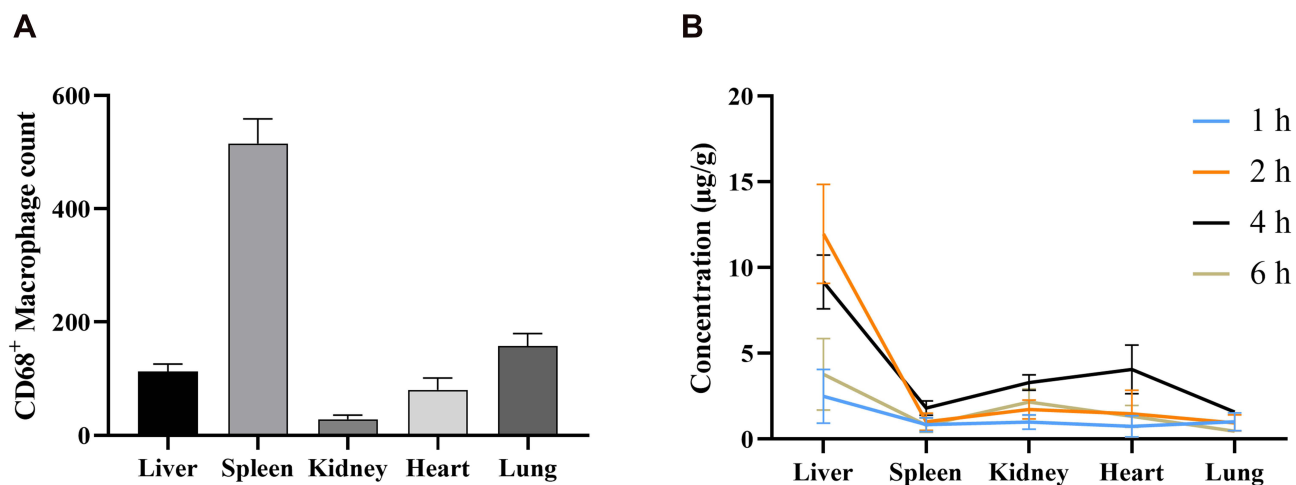
(Figure 9A). However, the concentrations of BBR and OBB were the highest in the liver and nearly the lowest in the spleen within 6 h (Figure 9B). The levels of OBB and BBR in tissues were not linear simply to the number of CD68^{+} macrophages.

Evaluation of the Anti-Inflammatory Effect of BBR and Its Metabolite OBB
### Cytotoxic Effect of OBB and BBR on RAW264.7 Macrophages

To assess the potential cytotoxic effect of BBR and OBB on RAW 264.7 cells, diverse concentrations of BBR (2.5, 5, 10, 20, 40, 80 μM) and OBB (2.5, 5, 10, 20, 40, 80 μM) with or without LPS were used to incubate the cells for 24 h. As shown in Figure 10, the CCK8 assay indicated that OBB exhibited no significant inhibition on the growth of RAW 264.7 cells in the concentration ranging from 2.5 to 80 μM. However, BBR up to the concentration of 80 μM showed toxic effect on RAW 264.7 cells in parallel to the control cells. Besides, co-treatment with OBB and LPS showed no significant toxicity. The combination of BBR and LPS produced significant toxicity when the concentration of BBR reached above 40 μM.

Inflammatory Cytokine Production in RAW 264.7 Macrophages

As depicted in Figure 11A–C, stimulation of LPS upregulated dramatically the contents of pro-inflammation cytokines TNF-α, IL-6 and IL-18 in comparison to the control counterpart. OBB (0.1, 0.2 and 0.4 μM) significantly suppressed the

A

B

Figure 9 (**A**) The amount of CD68⁺ macrophages in different tissues of normal rats (n = 3). (**B**) The concentrations of BBR and OBB in tissues at 1, 2, 4 and 6 h (n = 6). Data are presented as mean ± S.E.M.

A

B

C

D
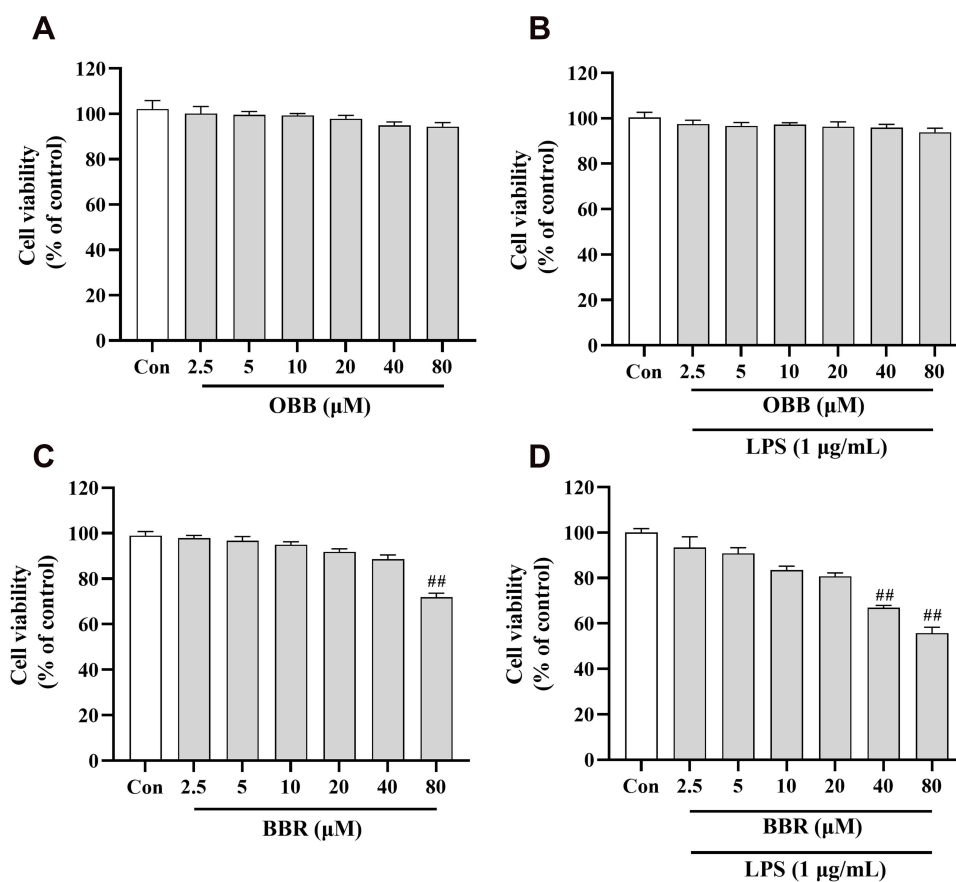
Figure 10 Cell viability of RAW 264.7 macrophages incubated with OBB and BBR with or without LPS (1 μg/mL) for 24 h. Cells were exposed to different drugs: (**A**) OBB, (**B**) OBB and LPS, (**C**) BBR, (**D**) BBR and LPS. The cell viability was determined by CCK8 assay. Data are presented as mean ± S.E.M. (n = 3). $^{###}p < 0.01$ vs the control group.

levels of TNF-α, IL-6, and IL-18. Of note, RAW 264.7 cells treated with 0.4 μM OBB resulted in significantly decreased levels of IL-6 and IL-18 as compared to those treated with BBR (5 μM). These results indicated that OBB might exert superior anti-inflammatory effect to BBR even at a low dose.
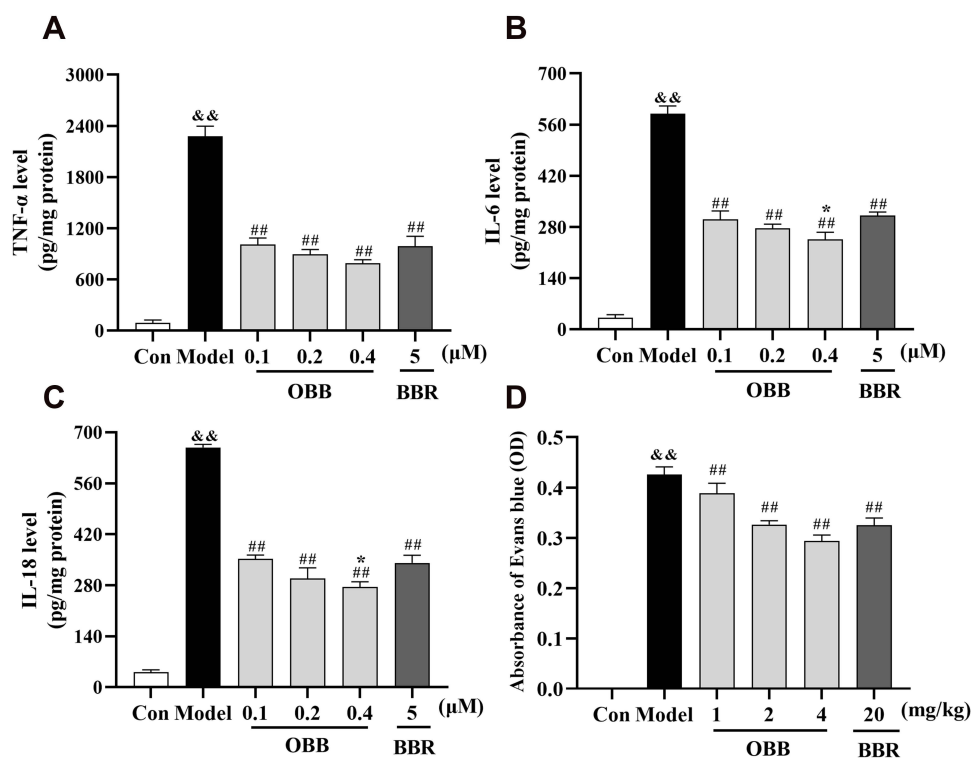
Figure 11 Comparison of anti-inflammatory effects between BBR and OBB in vitro and in vivo. (**A–C**) Effect of OBB on secretions of pro-inflammatory mediators TNF-α, IL-6, and IL-18 in LPS-induced RAW 264.7 macrophages. (n = 3). (**D**) Vascular permeability in mice induced by acetic acid. The capillary permeability was described by the content of Evans blue expelled into peritoneal cavity, which was measured by the OD of the supernatant (n = 10). Data are presented as mean ± S.E.M. [&&]$p < 0.01$ vs the Control group; [##]$p < 0.01$ vs the Model group; [*]$p < 0.05$ vs the BBR group.

Acetic Acid-Induced Vascular Permeability in Mice

As presented in Figure 11D, pretreatment with OBB (1, 2, 4 mg/kg) and BBR (20 mg/kg) significantly suppressed the vascular permeability in a dose-dependent manner compared to the model group. The inhibitory rates of OBB (1, 2, 4 mg/kg) and BBR (20 mg/kg) were 11.82%, 25.97%, 33.34% and 26.28%, respectively. The inhibitory effect of OBB at the dose of 2 mg/kg was as effective as that of BBR at the dose of 20 mg/kg.

Discussion

Berberine is a renowned alkaloid that has been documented to have various pharmacological activities. Due to the contradiction between its therapeutic effect and limited plasma concentration, BBR is always a hot issue in its biological and pathological processes. In terms of pharmacodynamics, the limited studies available mainly focused on the level of components in plasma,[20] while the study on the role of other major components in blood like erythrocyte is rare and insufficient. Erythrocytes, the most abundant blood cell type, occupy a quarter of the total cell numbers within the human body.[24] Erythrocytes harbor various distinctive properties such as unmatched long circulation, biocompatibility and biodegradability that make them appealing vascular carriers for in vivo delivery of natural and synthetic payloads.[9,25] Although our previous study has suggested a BBR erythrocytes-Hb self-assembly delivery system,[12] the metabolic aspect, targeted delivery and dose–effect relationship of BBR mediated by erythrocytes have not yet been clearly clarified.

It has been reported that BBR-erythrocytes delivery system has been developed artificially and erythrocytes served as delivery vehicles for BBR to achieve the long-acting hypolipidemic effect.[26] In our previous work, a BBR erythrocytes-Hb self-assembly delivery system has been identified and the accumulation of BBR in erythrocytes was attributed to the intense conjugation of BBR with Hb.[12] In this study, BBR achieved a significantly higher concentration in erythrocytes than in plasma in rats after intragastrical administration with PCC and intraperitoneal administration with BBR, which

was in agreement with our previous findings.[12,13] HCl, a hydrolyzing agent, could be used for the hydrolysis of drug-Hb adducts.[27] Incubation samples of BBR and whole blood (including plasma and erythrocytes) treated with HCl have been found to have a notable increase in BBR concentration. This observation indicated that BBR was present predominantly in erythrocytes and released from the Hb complex. Hence, erythrocytes, acting as the hidden carriers, could autonomously load and deliver BBR.

BBR has limited solubility and low absorption in the small intestine.[28] It has been acknowledged that an oral dose of 400 mg/kg BBR resulted in a maximum plasma concentration (C_{max}) of 0.4 ng/mL.[29] And the absolute bioavailability of BBR was less than 1%.[30,31] The contradiction between the explicit therapeutic effects of berberine and its very low plasma concentration promotes the hypothesis that the metabolites of berberine may substantially contribute to its biological activities.[32] As reported, 43.8% of BBR was metabolized[7] and it could be metabolized into 97 metabolites in rat,[33] which explained to some extent its low plasma concentration in vivo. However, studies on BBR metabolites have mainly concentrated on the common and easily found metabolites in the liver, such as berberrubine, demethyleneberberine, palmatine, jatrorrhizine and thalifendine,[20,34–37] the pharmacokinetic profiles of other metabolites remained ambiguous.

In addition to functioning as a drug carrier, erythrocytes also serve as metabolic site. Erythrocyte metabolism, independent of hepatic and gastric metabolism, is a frequently overlooked metabolic pathway. Erythrocytes are the transporters of oxygen and contain reactive oxygen species which may cause oxidative metabolism of drugs.[14,38] Similarly, the accumulation of hydrogen peroxide in erythrocytes was considered to account for the formation of a metabolite. Furthermore, Hb was expected to achieve catalytic reactions with selectivity from the interaction of the substrate with a natural, evolvable binding site.[39,40] However, the metabolic function of erythrocytes for drugs has not received sufficient attention. In our previous work, OBB, one of the metabolites of BBR, has been found to be transformed from BBR via erythrocyte metabolism either in vivo or in vitro in our previous work.[41] Therefore, in addition to metabolism in the liver and intestine, erythrocytes might perform an important role in the metabolism of BBR by predominating oxidative reaction pathway.

OBB has been reported to possess superior anti-arrhythmic, antifungal and antitumor activities to BBR in previous studies.[42–44] In our recent study, OBB has been observed to exhibit superior bioactivities with more favorable safety profile.[19,45,46] Furthermore, OBB has been found to exist in the whole blood in the Hb-bound form in rats after intravenous injection with BBR.[13] In this follow-up study, we further endeavored to investigate the conversion rate of BBR into OBB and the erythrocytes/plasma partition coefficient, an important parameter for drug distribution and the physiological interpretation. The result obtained indicated that more than 80% of BBR underwent rapid oxidation in erythrocytes with only a very small portion (8.61%) of BBR remaining in plasma in the first half-hour. When the prodrug BBR was bio-transformed to its oxidized congener OBB, the C-8 quaternary ammonium structure was converted to a more active lactam ring. The lipophilicity and absorbance of OBB would expectedly be elevated for easier ferry through biological membranes, which potentially resulted in the enhancement of its bioactivity.

In this study, OBB exhibited similar anti-inflammatory effect as BBR at an approximately 10-fold lower dose (0.1 μM). TNF-α and IL-6 potentially act as mediators of precise control and induction of inflammation, immune response and viral infection.[47,48] Besides, IL-18 is also positively related to systemic inflammation and liver injury.[49,50] They are the common proinflammatory cytokines which are released mainly by the hepatic macrophages/Kupffer cells via the activation of the inflammasome. The anti-inflammatory effects of OBB and BBR were potentially associated with inhibition of pro-inflammatory factors (TNF-α, IL-6 and IL-18) and inflammatory response. The pharmacokinetic studies showed that the level of OBB in vivo was more than 0.1 μM, which was sufficient to exert appreciable anti-inflammatory effect. The acetic acid-induced vascular permeability assay is a renowned model for evaluating inflammatory processes. Acetic acid intensifies various mediators (histamine, prostaglandins and 5-hydroxytryptamine) in the peritoneal cavity, causing dilation of capillaries and increasing vascular permeability.[51] Our result indicated that OBB exhibited a significant inhibitory effect in a dose-dependent manner on vascular permeability in mice. Of note, the dose of OBB (approximately one-quarter of BBR dose) that showed efficacy was much less than that of BBR. This correlation observed indicated that the anti-inflammatory effect of BBR might be attributed, at least partially, to its active metabolite OBB.

Besides loading the drugs and metabolizing them into the more active metabolite, targeted delivery of these molecules to specific organs is an important feature of erythrocytes.[52] To effectively achieve in situ loading of circulating drugs for therapy, the intrinsic phagocytic behavior of monocytes/macrophages is utilized to specifically engulf some endogenous substances in blood stream.[53] Natural damaging/aging erythrocytes, which are regarded as blood waste materials, are specifically phagocytized and eliminated by monocytes/macrophages. This process is called erythrophagocytosis.[54] Promisingly, the artificially damaging/senescent erythrocytes can also mimic the natural morphological, immunological and biochemical properties of damaged/aging erythrocytes and could be exploited to hitchhik on circulating monocytes/macrophages for the accumulation of drugs.

Autogenous drug-loaded erythrocytes, which are deemed as the damaged cells, deplete monocytes/macrophages by inducing apoptosis in the monocytes/macrophages that engulf them.[55,56] It has been covered that engineered erythrocytes were employed as vehicles to deliver target drugs to the macrophages.[55,57,58] For example, to optimize the bioavailability and selectivity of the insoluble drugs to active phagocytes and other components of the immune system in the mono-nuclear phagocyte systems (MPS), the delivery of erythrocytes-loaded anti-inflammatory drugs (eg, glucocorticoids) to pro-inflammatory cells (such as macrophages) has been conducted.[59] In the present study, it was interesting to note that there was a strong positive linear correlation between drug concentration in erythrocytes and monocyte depletion. By increasing the intracellular drug concentration in erythrocytes, the ability of drug-loaded erythrocytes to promote macrophage phagocytosis increased as well, which might cause a decrease in monocytes number in the peripheral blood.

Tissue distribution of BBR and OBB, particularly in certain target organs and the active sites in vivo, could also serve as evidence of drug-loading erythrocytes targeting macrophages. In our study, dominant tissue distribution of BBR and OBB was observed in the liver. The delivery of BBR to circulating monocytes/macrophages encountered the phagocytic cells of the liver (mainly Kupffer cells). The drug-loaded erythrocytes were naturally scavenged by hepatic reticuloendothelial system (RES) macrophages (Kupffer cells), subsequently broken down in the lysosome, and caused the release and accumulation of drugs in the tissues rich in macrophages (such as liver).[41,55,56,60]

In theory, the spleen, the biggest immunity organ and the center of cellular immunity and humor immunity, contains numerous macrophages[61] and is considered the highest uptake organ of BBR. However, the concentration of BBR in the spleen was the lowest in comparison to the other tissues. The reason behind this phenomenon might be associated with the physiology of the liver. Indeed, the liver is mainly supplied by the portal vein which transports the blood from the mesenteric venous. Therefore, drug-loaded erythrocytes reach mostly the liver where they are engulfed by Kupffer cells after intragastric administration. Such blood, poor in drug-loaded erythrocytes with the hepatic first-pass effect, subsequently flows to the other tissues through hepatic vein and then enters the blood circulation. Therefore, fewer drug-loaded erythrocytes are available to deplete macrophages of organs except for the liver. The pharmacokinetic characteristics of BBR observed and drug-delivery through phagocytosis in the RES mediated by erythrocytes might result in minimization of drug-mediated toxic effects upon nonphagocytic cells with favorable safety profile in vivo.

As summarized in Figure 12, in this paper, we indicated 1) that BBR was largely present in erythrocytes in vivo after oral administration of PCC, 2) that BBR entered erythrocytes and was metabolized to OBB after intraperitoneal injection of BBR in rats, 3) that a negative correlation was observed between total concentrations of BBR and OBB in erythrocytes and monocyte depletion in peripheral blood, and 4) that OBB exhibited similar anti-inflammatory activity as BBR with a much lower dosage in vivo and in vitro.

Taken together, erythrocytes might unintentionally represent the carrier critically participating in biodistribution, pharmacokinetics, metabolism and target delivery of BBR/OBB into phagocytic cells. The results might interpret the mystery of the extremely low plasma concentration of BBR, and reveal the hidden and critical role of erythrocytes as the simultaneous metabolic reservoir and targeted vehicle for metabolizing and circulating BBR. The present study provided evidence to support that the anti-inflammatory activity of BBR and PCC was attributable, to a large extent, to the unique and indispensable roles of erythrocytes. It provides a novel dimension to explain the paradox between the poor bioavailability and high efficacy of some low-soluble drugs. The natural erythrocytes self-assembling delivery system might serve a non-negligible role in exploring the pharmacokinetics–pharmacodynamics relationship of natural products.
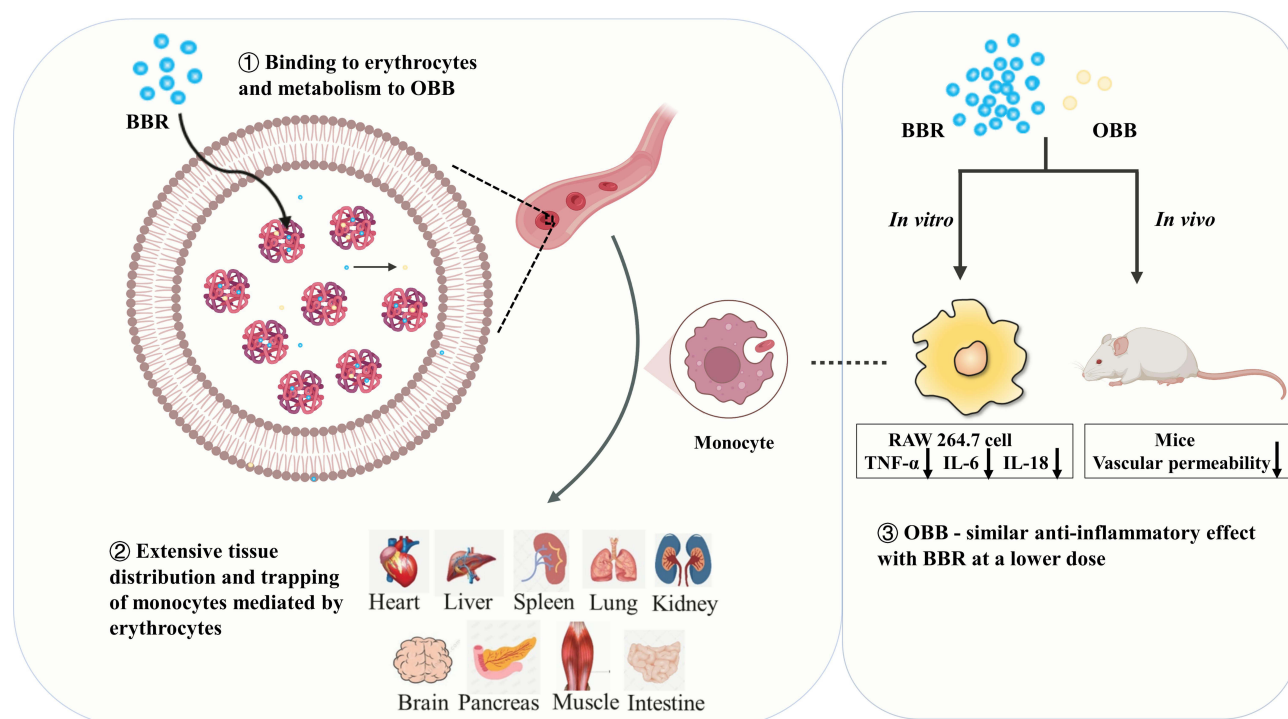
Figure 12 Summary scheme of the scenario for the pharmacokinetics and anti-inflammatory pharmacodynamics of BBR and its active metabolite OBB from the perspective of BBR-erythrocytes self-assembly delivery system.

Conclusion

In conclusion, BBR was prodominantly found in erythrocytes, which critically participated in the biodistribution, pharmacokinetics, metabolism and target delivery of BBR and its metabolite. The anti-inflammatory activity of BBR and PCC was intimately associated with the metabolism into the active congener OBB and the targeted delivery to monocytes/macrophages mediated by the erythrocytes.

Abbreviations

BBR, berberine; ELISA, enzyme-linked immunosorbent assay; Hb, hemoglobin; HPLC, high-performance liquid chromatography; IL-18, interleukin-18; IL-6, interleukin-6; LPS, lipopolysaccharide; OBB, oxyberberine; PCC, Phellodendri Chinensis Cortex; RES, reticuloendothelial system; TNF-α, tumor necrosis factor alpha.

Acknowledgments

Author Contributions

All authors made a significant contribution to the work reported, whether that is in the conception, study design, execution, acquisition of data, analysis and interpretation, or in all these areas; took part in drafting, revising or critically reviewing the article; gave final approval of the version to be published; have agreed on the journal to which the article has been submitted; and agree to be accountable for all aspects of the work.

Disclosure

The authors declared that there was no potential conflict of interest.

References

1. Committee CP. *Pharmacopeia of the People's Republic of China (The First Division)*. Chinese Medical Science and Technology Press; 2020:318.

2. Chen G, Li KK, Fung CH, et al. Er-Miao-San, a traditional herbal formula containing Rhizoma Atractylodis and Cortex Phellodendri inhibits inflammatory mediators in LPS-stimulated RAW264.7 macrophages through inhibition of NF-κB pathway and MAPKs activation. *J Ethnopharmacol*. 2014;154(3):711–718. doi:10.1016/j.jep.2014.04.042

3. Xian YF, Mao QQ, Ip SP, Lin ZX, Che CT. Comparison on the anti-inflammatory effect of cortex phellodendri chinensis and cortex phellodendri amurensis in 12-O-tetradecanoyl-phorbol-13-acetate-induced ear edema in mice. *J Ethnopharmacol*. 2011;137(3):1425–1430. doi:10.1016/j.jep.2011.08.014

4. Li Q, Huang Z, Liu D, et al. Effect of berberine on hyperuricemia and kidney injury: a network pharmacology analysis and experimental validation in a mouse model. *Drug Des Devel Ther*. 2021;15:3241–3254. doi:10.2147/dddt.S317776

5. Zhu L, Gu P, Shen H. Protective effects of berberine hydrochloride on DSS-induced ulcerative colitis in rats. *Int Immunopharmacol*. 2019;68:242–251. doi:10.1016/j.intimp.2018.12.036

6. Liu SC, Lee HP, Hung CY, Tsai CH, Li TM, Tang CH. Berberine attenuates CCN2-induced IL-1β expression and prevents cartilage degradation in a rat model of osteoarthritis. *Toxicol Appl Pharmacol*. 2015;289(1):20–29. doi:10.1016/j.taap.2015.08.020

7. Liu YT, Hao HP, Xie HG, et al. Extensive intestinal first-pass elimination and predominant hepatic distribution of berberine explain its low plasma levels in rats. *Drug Metab Dispos*. 2010;38(10):1779–1784. doi:10.1124/dmd.110.033936

8. Liu CS, Zheng YR, Zhang YF, Long XY. Research progress on berberine with a special focus on its oral bioavailability. *Fitoterapia*. 2016;109:274–282. doi:10.1016/j.fitote.2016.02.001

9. Patel PD, Dand N, Hirlekar RS, Kadam VJ. Drug loaded erythrocytes as novel drug delivery system. *Curr Pharm Des*. 2008;14:63–70. doi:10.2174/138161208783330772

10. Alayash AI. Hemoglobin oxidation reactions in stored blood. *Antioxidants*. 2022;11(4). doi:10.3390/antiox11040747

11. Garcia RA, Bumanlag LP, Piazza GJ. The relationship between extent of hemoglobin purification and the performance characteristics of a blood-based flocculant. *J Sci Food Agric*. 2017;97(14):4822–4826. doi:10.1002/jsfa.8352

12. Yu Q, Li M, Chen H, et al. The discovery of berberine erythrocyte-hemoglobin self-assembly delivery system: a neglected carrier underlying its pharmacokinetics. *Drug Deliv*. 2022;29(1):856–870. doi:10.1080/10717544.2022.2036870

13. Chen HB, Luo CD, Ai GX, et al. A comparative investigation of the interaction and pharmacokinetics of hemoglobin with berberine and its oxymetabolite. *J Pharm Biomed Anal*. 2021;199:114032. doi:10.1016/j.jpba.2021.114032

14. Fasinu PS, Nanayakkara NPD, Wang YH, et al. Formation primaquine-5,6-orthoquinone, the putative active and toxic metabolite of primaquine via direct oxidation in human erythrocytes. *Malar J*. 2019;18(1):30. doi:10.1186/s12936-019-2658-5

15. Pan H, Gu L, Sun S, et al. Metabolism of bis(4-fluorobenzyl)trisulfide and its formation of hemoglobin adduct in rat erythrocytes. *Drug Metab Dispos*. 2013;41(5):1082–1093. doi:10.1124/dmd.112.048801

16. Fan NC, Cheng FY, Ho JA, Yeh CS. Photocontrolled targeted drug delivery: photocaged biologically active folic acid as a light-responsive tumor-targeting molecule. *Angew Chem Int Ed Engl*. 2012;51(35):8806–8810. doi:10.1002/anie.201203339

17. Zhang Y, Wang Y, Xin Q, et al. Zwitterionic choline phosphate conjugated folate-poly (ethylene glycol): a general decoration of erythrocyte membrane-coated nanoparticles for enhanced tumor-targeting drug delivery. *J Mater Chem B*. 2022. doi:10.1039/d1tb02493k

18. Zheng J, Lu C, Ding Y, et al. Red blood cell-hitchhiking mediated pulmonary delivery of ivermectin: effects of nanoparticle properties. *Int J Pharm*. 2022;619:121719. doi:10.1016/j.ijpharm.2022.121719

19. Li C, Ai G, Wang Y, et al. Oxyberberine, a novel gut microbiota-mediated metabolite of berberine, possesses superior anti-colitis effect: impact on intestinal epithelial barrier, gut microbiota profile and TLR4-MyD88-NF-κB pathway. *Pharmacol Res*. 2020;152:104603. doi:10.1016/j.phrs.2019.104603

20. Wang Z, Song M, Cui B, et al. A LC-MS/MS method for simultaneous determination of seven alkaloids in rat plasma after oral administration of Phellodendri chinensis cortex extract and its application to a pharmacokinetic study. *J Sep Sci*. 2019;42(7):1351–1363. doi:10.1002/jssc.201801018

21. Maimaiti Z, Xu C, Fu J, Chai W, Zhou Y, Chen J. The potential value of monocyte to lymphocyte ratio, platelet to mean platelet volume ratio in the diagnosis of periprosthetic joint infections. *Orthop Surg*. 2021;14:306–314. doi:10.1111/os.12992

22. Wu Y, Huang S, Xiao S, He J, Lu F. Impact of galectin-receptor interactions on liver pathology during the erythrocytic stage of plasmodium berghei malaria. *Front Immunol*. 2021;12:758052. doi:10.3389/fimmu.2021.758052

23. Zhang Z, Li L, Huang G, et al. Embelia Laeta aqueous extract suppresses acute inflammation via decreasing COX-2/iNOS expression and inhibiting NF-kappaB pathway. *J Ethnopharmacol*. 2021;281:114575. doi:10.1016/j.jep.2021.114575

24. Yang Y, Chen J, Lu L, et al. The antibacterial activity of erythrocytes from goose (anser domesticus) can be associated with phagocytosis and respiratory burst generation. *Front Immunol*. 2021;12:766970. doi:10.3389/fimmu.2021.766970

25. Muzykantov VR. Drug delivery by red blood cells: vascular carriers designed by mother nature. *Expert Opin Drug Deliv*. 2010;7(4):403–427. doi:10.1517/17425241003610633

26. Cheng Z, Liu S, Wu X, et al. Autologous erythrocytes delivery of berberine hydrochloride with long-acting effect for hypolipidemia treatment. *Drug Deliv*. 2020;27(1):283–291. doi:10.1080/10717544.2020.1716880

27. Busquets R, Puignou L, Galceran MT. Determination of 2-amino-1-methyl-6-phenylimidazo[4,5-b]pyridine (PhIP) in hemoglobin using on-line coupling of restricted access material to liquid chromatography–mass spectrometry. *Anal Chim Acta*. 2006;559(1):45–53. doi:10.1016/j.aca.2005.11.052

28. Javed Iqbal M, Quispe C, Javed Z, et al. Nanotechnology-based strategies for berberine delivery system in cancer treatment: pulling strings to keep berberine in power. *Front Mol Biosci*. 2020;7:624494. doi:10.3389/fmolb.2020.624494

29. Hua W, Ding L, Chen Y, Gong B, He J, Xu G. Determination of berberine in human plasma by liquid chromatography-electrospray ionization-mass spectrometry. *J Pharm Biomed Anal*. 2007;44(4):931–937. doi:10.1016/j.jpba.2007.03.022

30. Chen W, Miao YQ, Fan DJ, et al. Bioavailability study of berberine and the enhancing effects of TPGS on intestinal absorption in rats. *AAPS PharmSciTech*. 2011;12(2):705–711. doi:10.1208/s12249-011-9632-z

31. Feng X, Wang K, Cao S, Ding L, Qiu F. Pharmacokinetics and excretion of berberine and its nine metabolites in rats. *Front Pharmacol*. 2020;11:594852. doi:10.3389/fphar.2020.594852

32. Wang K, Feng X, Chai L, Cao S, Qiu F. The metabolism of berberine and its contribution to the pharmacological effects. *Drug Metab Rev*. 2017;49(2):139–157. doi:10.1080/03602532.2017.1306544

33. Wang K, Chai L, Feng X, et al. Metabolites identification of berberine in rats using ultra-high performance liquid chromatography/quadrupole time-of-flight mass spectrometry. *J Pharm Biomed Anal*. 2017;139:73–86. doi:10.1016/j.jpba.2017.02.038

34. Zhang ZW, Cong L, Peng R, et al. Transformation of berberine to its demethylated metabolites by the CYP51 enzyme in the gut microbiota. *J Pharm Anal*. 2021;11(5):628–637. doi:10.1016/j.jpha.2020.10.001

35. Zhou Y, Cao S, Wang Y, et al. Berberine metabolites could induce low density lipoprotein receptor up-regulation to exert lipid-lowering effects in human hepatoma cells. *Fitoterapia*. 2014;92:230–237. doi:10.1016/j.fitote.2013.11.010

36. Tan XS, Ma JY, Feng R, et al. Tissue distribution of berberine and its metabolites after oral administration in rats. *PLoS One*. 2013;8(10):e77969. doi:10.1371/journal.pone.0077969

37. Zuo F, Nakamura N, Akao T, Hattori M. Pharmacokinetics of berberine and its main metabolites in conventional and pseudo germ-free rats determined by liquid chromatography/ion trap mass spectrometry. *Drug Metab Dispos*. 2006;34(12):2064–2072. doi:10.1124/dmd.106.011361

38. Hsia CC. Respiratory function of hemoglobin. *N Engl J Med*. 1998;338(4):239–247. doi:10.1056/nejm199801223380407

39. Key HM, Dydio P, Clark DS, Hartwig JF. Abiological catalysis by artificial haem proteins containing noble metals in place of iron. *Nature*. 2016;534(7608):534–537. doi:10.1038/nature17968

40. Zhang K, Mao L, Cai R. Stopped-flow spectrophotometric determination of hydrogen peroxide with hemoglobin as catalyst. *Talanta*. 2000;51:179–186. doi:10.1016/S0039-9140(99)00277-5

41. Kondo H, Saito K, Grasso JP, Aisen P. Iron metabolism in the erythrophagocytosing Kupffer cell. *Hepatology*. 1988;8:32–38. doi:10.1002/hep.1840080108

42. Chi JF, Chu SH, Lee CS, Chou NK, Su MJ. Mechanical and electrophysiological effects of 8-oxoberberine (JKL1073A) on atrial tissue. *Br J Pharmacol*. 1996;118(3):503–512. doi:10.1111/j.1476-5381.1996.tb15431.x

43. Singh S, Verma M, Malhotra M, Prakash S, Singh TD. Cytotoxicity of alkaloids isolated from Argemone mexicana on SW480 human colon cancer cell line. *Pharm Biol*. 2016;54(4):740–745. doi:10.3109/13880209.2015.1073334

44. Singh A, Singh S, Singh S, et al. Fungal spore germination inhibition by alkaloids dehydrocorydalmine and oxyberberine. *J Plant Prot Res*. 2009;49(3):287–289. doi:10.2478/v10045-009-0046-9

45. Li Q, Dou YX, Huang ZW, et al. Therapeutic effect of oxyberberine on obese non-alcoholic fatty liver disease rats. *Phytomedicine*. 2021;85:153550. doi:10.1016/j.phymed.2021.153550

46. Dou Y, Huang R, Li Q, et al. Oxyberberine, an absorbed metabolite of berberine, possess superior hypoglycemic effect via regulating the PI3K/Akt and Nrf2 signaling pathways. *Biomed Pharmacother*. 2021;137:111312. doi:10.1016/j.biopha.2021.111312

47. Isorce N, Testoni B, Locatelli M, et al. Antiviral activity of various interferons and pro-inflammatory cytokines in non-transformed cultured hepatocytes infected with hepatitis B virus. *Antiviral Res*. 2016;130:36–45. doi:10.1016/j.antiviral.2016.03.008

48. Ghavami SB, Mohebbi SR, Karimi K, et al. Variants in two gene members of the TNF ligand superfamily and hepatitis C virus chronic disease. *Gastroenterol Hepatol Bed Bench*. 2018;11(Suppl 1):S66–S72. PMID: 30774809.

49. Yasuda K, Nakanishi K, Tsutsui H. Interleukin-18 in health and disease. *Int J Mol Sci*. 2019;20:(3)649. doi:10.3390/ijms20030649

50. Flisiak-Jackiewicz M, Bobrus-Chociej A, Tarasow E, Wojtkowska M, Bialokoz-Kalinowska I, Lebensztejn DM. Predictive role of interleukin-18 in liver steatosis in obese children. *Can J Gastroenterol Hepatol*. 2018;2018:20183870454. doi:10.1155/2018/3870454

51. Liu N, Zhang GX, Niu YT, et al. Anti-inflammatory and analgesic activities of indigo through regulating the IKKbeta/IkappaB/NF-kappaB pathway in mice. *Food Funct*. 2020;11(10):8537–8546. doi:10.1039/c9fo02574j

52. Yamamura T, Horinouchi T, Adachi T, et al. Development of an exon skipping therapy for X-linked Alport syndrome with truncating variants in COL4A5. *Nat Commun*. 2020;11(1):2777. doi:10.1038/s41467-020-16605-x

53. Zheng L, Hu X, Wu H, et al. In vivo monocyte/macrophage-hitchhiked intratumoral accumulation of nanomedicines for enhanced tumor therapy. *J Am Chem Soc*. 2020;142(1):382–391. doi:10.1021/jacs.9b11046

54. Recalcati S, Macrophages CG. Iron: a special relationship. *Biomedicines*. 2021;9(11):1585. doi:10.3390/biomedicines9111585

55. Feng Y, Liu Q, Li Y, et al. Cell relay-delivery improves targeting and therapeutic efficacy in tumors. *Bioact Mater*. 2021;6(6):1528–1540. doi:10.1016/j.bioactmat.2020.11.014

56. Simmons WR, Wain L, Toker J, et al. Normal iron homeostasis requires the transporter SLC48A1 for efficient heme-iron recycling in mammals. *Front Genome Ed*. 2020;2:8. doi:10.3389/fgeed.2020.00008

57. Sabatino R, Antonelli A, Battistelli S, Schwendener R, Magnani M, Rossi L. Macrophage depletion by free bisphosphonates and zoledronate-loaded red blood cells. *PLoS One*. 2014;9(6):e101260. doi:10.1371/journal.pone.0101260

58. Pina Y, Boutrid H, Murray TG, et al. Impact of tumor-associated macrophages in LH(BETA)T(AG) mice on retinal tumor progression: relation to macrophage subtype. *Invest Ophthalmol Vis Sci*. 2010;51(5):2671–2677. doi:10.1167/iovs.09-4255

59. Rossi L, Castro M, D'Orio F, et al. Low doses of dexamethasone constantly delivered by autologous erythrocytes slow the progression of lung disease in cystic fibrosis patients. *Blood Cells Mol Dis*. 2004;33(1):57–63. doi:10.1016/j.bcmd.2004.04.004

60. Tanei T, Leonard F, Liu X, et al. Redirecting transport of nanoparticle albumin-bound paclitaxel to macrophages enhances therapeutic efficacy against liver metastases. *Cancer Res*. 2016;76(2):429–439. doi:10.1158/0008-5472.CAN-15-1576

61. Fan J, Zhuang Y, Li B. Effects of collagen and collagen hydrolysate from jellyfish umbrella on histological and immunity changes of mice photoaging. *Nutrients*. 2013;5(1):223–233. doi:10.3390/nu5010223

Drug Design, Development and Therapy

Dovepress

Publish your work in this journal